

Discovery potential of the NMSSM CP-odd Higgs at the LHC

M. Almarashi¹

Departement of Physics, Taibah University, Almadinah, KSA

Abstract

In this paper we examine the LHC discovery potential of the lightest CP-odd Higgs boson, a_1 , of the NMSSM produced in gluon fusion channel $gg \rightarrow a_1$. We evaluate the inclusive signal rates of the a_1 for a variety of decay channels and discuss its possible discovery. It is observed that the overall production and decay rates at inclusive level are quite sizable and should help extracting the a_1 signal over some regions of the NMSSM parameter space.

1 Introduction

The observation of a Higgs signal at the LHC [1–4] in 2012 is considered a huge success of the Standard Model (SM). Although its measured properties agrees with the SM predictions, the Higgs-like particle can be embedded in Supersymmetric models. In its minimal realisation, the so-called Minimal Supersymmetric Standard Model (MSSM), the SM is extended by introducing two Higgs doublets instead of the one in the SM, giving rise to five physical Higgs states: two CP-even Higgses, h and H ($m_h < m_H$), one CP-odd Higgs, A , and a pair of charged Higgses H^\pm instead of the only one in the SM. However, the MSSM suffers from two serious flaws. The first one is the so-called μ -problem [5] and the second one is the little hierarchy problem [6, 7]. The above two problems of the MSSM can be solved by expanding its Higgs sector by introducing an additional Higgs singlet superfield in addition to the two MSSM-type Higgs doublets. This new model is called the Next-to-Minimal Supersymmetric Standard Model (NMSSM) [8]. Interestingly, this model can easily accommodate the the measured value of the SM-like Higgs boson mass around 125 GeV without much fine-tuning [9–22].

In the NMSSM, the soft Supersymmetry (SUSY)-breaking potential of the Higgs sector is described by the following Lagrangian contribution

$$V_{\text{NMSSM}} = m_{H_u}^2 |H_u|^2 + m_{H_d}^2 |H_d|^2 + m_S^2 |S|^2 + \left(\lambda A_\lambda S H_u H_d + \frac{1}{3} \kappa A_\kappa S^3 + \text{h.c.} \right), \quad (1)$$

¹mmarashi@taibahu.edu.sa

where H_u and H_d are the Higgs doublet fields, S is the singlet one, λ and κ are Yukawa coupling parameters while A_λ and A_κ are dimensionful parameters of the order of SUSY mass scale M_{SUSY} .

The NMSSM Higgs sector at the tree-level is described by six independent parameters: κ , A_κ , λ , A_λ , $\tan\beta$ (the ratio of the vacuum expectation values (VEVs) of the two Higgs doublets) and $\mu_{\text{eff}} = \lambda\langle S \rangle$ (where $\langle S \rangle$ is the VEV of the singlet field). Assuming CP-conservation in the Higgs sector, the NMSSM contains seven Higgs states: three CP-even Higgses $h_{1,2,3}$ ($m_{h_1} < m_{h_2} < m_{h_3}$), two CP-odd Higgses $a_{1,2}$ ($m_{a_1} < m_{a_2}$) and a pair of charged Higgses h^\pm . Consequently, the Higgs sector of the NMSSM is phenomenologically richer than that of the MSSM. Further, when the scalar component of the singlet field acquires a non-vanishing vacuum expectation value, the μ -term in the superpotential will be dynamically generated, thus solving the μ -problem [23].

In the NMSSM, a_1 state is a composition of the usual doublet component of the CP-odd MSSM Higgs boson, a_{MSSM} , and the new singlet component, a_S , coming from the singlet superfield of the NMSSM. This can be written as [24]:

$$a_1 = a_{\text{MSSM}} \cos \theta_A + a_S \sin \theta_A, \quad (2)$$

where $\cos \theta_A$ and $\sin \theta_A$ are the mixing angles. When $\cos \theta_A$ goes to zero, the a_1 is highly singlet. To a good approximation the m_{a_1} can be written as:

$$m_{a_1}^2 = \frac{9A_\lambda\mu_{\text{eff}}}{2\sin 2\beta} \cos^2 \theta_A - 3\frac{\kappa A_\kappa\mu_{\text{eff}}}{\lambda} \sin^2 \theta_A. \quad (3)$$

It is clear from the last equation that all the tree level parameters of the NMSSM Higgs sector jointly affects m_{a_1} in general.

There have been some studies exploring the production potential of the NMSSM CP-odd Higgs states at the LHC and other colliders [25–39]. It was found that the best direct production channel of producing the lightest CP-odd Higgs state a_1 is through its production in association with a bottom antibottom pair $b\bar{b}a_1$. However, there is still no a comprehensive study about the detectability of the CP-odd Higgs particles at the LHC in gluon fusion production channel $gg \rightarrow a$.

In this paper, we explore the discovery potential of the a_1 at the LHC by looking for its direct production rather than looking for its traditional production through $h_{1,2}$ decay. We examine the discovery potential of the a_1 produced in gluon fusion channel $gg \rightarrow a_1$ through a variety of decay modes. We will estimate the inclusive cross section of the a_1 production to examine whether or not there exist some parameter space where the a_1 can be discovered at the LHC although detail analysis of the background is required to make a conclusive decision. It is shown that there is some regions of the NMSSM parameter space where the cross sections times branching ratio rates are quite remarkable for some decay channels and can be useful to look for the a_1 signals at the LHC through the above production channel.

The plan of this paper is as follows. In section 2 we describe the parameter space scans performed in the context of the NMSSM and discuss the allowed decay channels of the a_1 . In section 3 we present the inclusive event rates of a_1 production at the LHC for various decay channels. Finally, we summarize our results in section 4.

2 Exploring the NMSSM Parameter Space

For our study of the NMSSM Higgs sector we have used the package NMSSMTools5.1.2 [40–42] for the calculation of the branching ratios and spectrum of Higgs bosons and SUSY particles of the NMSSM. The package systematically takes into account various theoretical and experimental constraints.

We have used the above package to scan over some regions of the NMSSM parameter space in order to obtain a general view of the phenomenology of the lightest CP-odd Higgs boson, a_1 , at the LHC. We have set the six tree level parameters in the following ranges:

$$0.001 \leq \lambda \leq 0.7, \quad -0.65 \leq \kappa \leq 0.65, \quad 1.6 \leq \tan \beta \leq 60, \\ 100 \leq \mu \leq 1000 \text{ GeV}, \quad -2000 \leq A_\lambda \leq 2000 \text{ GeV}, \quad -20 \leq A_\kappa \leq 20 \text{ GeV}.$$

Notice that we have chosen the small values of A_κ to obtain small values of the m_{a_1} . Remaining soft SUSY breaking right- and left-handed masses for the first two generations and for the third generation, soft SUSY breaking trilinear couplings and gaugino soft SUSY breaking masses, contributing at higher order level, have been set as:

- $m_Q = m_U = m_D = m_L = m_E = 1 \text{ TeV}$,
- $m_{Q_3} = m_{U_3} = m_{D_3} = m_{L_3} = m_{E_3} = 1 \text{ TeV}$,
- $A_{U_3} = A_{D_3} = A_{E_3} = -2 \text{ TeV}$,
- $M_1 = 150 \text{ GeV}$, $M_2 = 300 \text{ GeV}$, $M_3 = 1 \text{ TeV}$.

The interesting decay channels which may help to discover the lightest CP-odd neutral Higgs boson a_1 at the LHC are:

$$a_1 \rightarrow \mu^+ \mu^-, \tau^+ \tau^-, gg, s\bar{s}, c\bar{c}, b\bar{b}, t\bar{t}, \gamma\gamma, Z\gamma, \text{ sparticles.} \quad (4)$$

We have performed a random scan over one million points in the specified parameter space. The scan output contains masses, branching ratios and couplings of the NMSSM Higgses and SUSY particles for all the surviving points which have passed the various experimental and theoretical constraints.

3 Higgs boson Signal Rates

In order to investigate the discovery potential of the a_1 at the LHC, we have computed the inclusive production rates by multiplying the NMSSM gluon fusion production cross section using CalcHEP [43] with the branching ratios computed with the NMSSMTools for all surviving data points ².

Figure 1 shows the production rates in femtobarn (fb) for the a_1 in the $\tau^+\tau^-$ and $\mu^+\mu^-$ final states, $\sigma(gg \rightarrow a_1) \text{ Br}(a_1 \rightarrow \tau^+\tau^-)$ and $\sigma(gg \rightarrow a_1) \text{ Br}(a_1 \rightarrow \mu^+\mu^-)$, as functions of m_{a_1} and of the corresponding branching ratios. As expected, the signal rate decreases with increasing m_{a_1} , see the left-panels of the figure. Also, it is remarkable to notice that the signal rates into $\tau^+\tau^-$ and $\mu^+\mu^-$ are sizable, topping the $7.3 \times 10^5 \text{ fb}$ and $2.8 \times 10^3 \text{ fb}$ levels

²We assume a centre-of-mass energy $\sqrt{s} = 14 \text{ TeV}$ for the LHC.

for $\tau^+\tau^-$ and $\mu^+\mu^-$ final states, respectively, for small values of m_{a_1} and decreasing rapidly with increasing m_{a_1} (left-panels). Further, it is clear that the rate into $\mu^+\mu^-$ final state shows the same pattern as the ones into $\tau^+\tau^-$ but is suppressed by a factor of $\approx (m_\mu^{\text{pole}}/m_\tau^{\text{pole}})^2$. Also, notice that $\text{Br}(a_1 \rightarrow \tau^+\tau^-)$ and $\text{Br}(a_1 \rightarrow \mu^+\mu^-)$ reaches about 10% and 0.035%, respectively, in most of the parameter space that has $m_{a_1} \geq 10$ GeV, in which case the a_1 decay into $b\bar{b}$ is kinematically open and dominant. However, there is a few points with light a_1 , $m_{a_1} < 10$ GeV, yielding large $\text{Br}(a_1 \rightarrow \tau^+\tau^-)$ and $\text{Br}(a_1 \rightarrow \mu^+\mu^-)$ greater than 90% and 0.4%, respectively, see the right-panels of the figure ³.

Overall, the inclusive cross section $\sigma(gg \rightarrow a_1) \text{Br}(a_1 \rightarrow \tau^+\tau^-)$ is quite large, so the $\tau^+\tau^-$ decay channel could be a good channel to discover the a_1 at the LHC, assuming the double- or single-leptonic decay channels of the τ 's. As for the $\mu^+\mu^-$ final state, the rates $\sigma(gg \rightarrow a_1) \text{Br}(a_1 \rightarrow \mu^+\mu^-)$ is also remarkable for a_1 low mass. For example, for $m_{a_1} \sim 100$ GeV, one can have up to several thousands events in the $\mu^+\mu^-$ channel at 100 fb^{-1} integrated luminosity. Therefore, the $\mu^+\mu^-$ decay channel is a promising channel to discover a light a_1 .

The signal rates for a_1 decaying into $b\bar{b}$ and $t\bar{t}$ as functions of m_{a_1} and of the corresponding branching ratios are shown in figure 2. The top-left panel of the figure shows that the signal rate in the $b\bar{b}$ final state is quite large, as the rates are at nb level for $m_{a_1} \leq 100$ GeV and at fb level for $m_{a_1} \simeq 300$ GeV. Also, it is clear from the top-right panel of the figure that for most points of the NMSSM parameter space the a_1 dominantly decays into $b\bar{b}$ final states with branching fraction close to 90%. Although, the discovery of the a_1 through $b\bar{b}$ channel is challenging due to large backgrounds, the size of the inclusive cross section is large enough to discover the a_1 especially if the background can be successfully reduced to manageable levels. As for the top quark pair final states, the signal rates are small, below 1 fb level, see the bottom-panels of the figure. Therefore, we think that the a_1 production at the LHC through $t\bar{t}$ final state is challenging due to the smallness of the signal rate and its complicated final state ⁴.

Figure 3 shows the distribution of event rates $\sigma(gg \rightarrow a_1) \text{Br}(a_1 \rightarrow \gamma\gamma)$ and $\sigma(gg \rightarrow a_1) \text{Br}(a_1 \rightarrow Z\gamma)$ as functions of m_{a_1} and of the corresponding branching ratios $\text{Br}(a_1 \rightarrow \gamma\gamma)$ and of $\text{Br}(a_1 \rightarrow Z\gamma)$. It is remarkable to notice that the rates are quite large, reaching maximum rates of about several hundreds fb for $\gamma\gamma$ and several tens fb for $Z\gamma$ final states. This is quite interesting as such signal events may be detectable at planned LHC luminosities. Also, it is obvious that the $\text{Br}(a_1 \rightarrow \gamma\gamma)$ and $\text{Br}(a_1 \rightarrow Z\gamma)$ can be dominant in some regions of the NMSSM parameter space, see the right-panes of the figure. This occurs when the a_1 is mostly singlet-like with a very small doublet component, i.e. the mixing angle $\cos\theta_A$ is very small, see figure 4. Such a possibility emerges when the tree-level decay to fermion-antifermion are highly suppressed, and so the decays $a_1 \rightarrow \gamma\gamma$ and $a_1 \rightarrow Z\gamma$ are dominant, due to large contributions from chargino loops.

Higgs bosons decaying into supersymmetric particles could play important roles for

³Notice that the mass region below the $b\bar{b}$ threshold is severely constrained, see, e.g., Ref. [44] (and references therein).

⁴We do not study the inclusive production rates for the decays $a_1 \rightarrow s\bar{s}$, $a_1 \rightarrow c\bar{c}$ and $a_1 \rightarrow gg$ due to large QCD backgrounds and smallness of their production rates in general

searching for such bosons. For example, to study the possibility of the a_1 production to SUSY particles, we have calculated the inclusive signal rates for the a_1 decaying into the lightest neutralinos $\chi_1^0\chi_1^0$ and into charginos $\chi_1^+\chi_1^-$, see figure 5. It is shown that the maximum signal rates are a few tens for the former and a few fb for the latter. The right-panels of the figure show that the $\text{Br}(a_1 \rightarrow \chi_1^0\chi_1^0)$ and $\text{Br}(a_1 \rightarrow \chi_1^+\chi_1^-)$ can be dominant in large regions of the NMSSM parameter space due to the enhancement of a_1 couplings with singlino-Higgsino components in χ_1^0 , χ_1^+ and χ_1^- states⁵. Notice that if the a_1 is highly singlet and its decays into $\chi_1^0\chi_1^0$ or into $\chi_1^+\chi_1^-$ are kinematically open, the $\text{Br}(a_1 \rightarrow \gamma\gamma)$ and $\text{Br}(a_1 \rightarrow Z\gamma)$ are no longer dominant, see figure 6, where the maximum values of both the $\text{Br}(a_1 \rightarrow \gamma\gamma)$ and $\text{Br}(a_1 \rightarrow Z\gamma)$ are $\leq 1\%$ (top-panels) and $\leq 0.01\%$ (bottom-panels), in which case the a_1 decay into $\chi_1^0\chi_1^0$ or into $a_1 \rightarrow \chi_1^+\chi_1^-$ becomes dominant.

Assuming R-parity is conserved, the lightest Supersymmetric particle (LSP) could be the lightest neutralino χ_1^0 in large regions of the parameter space of the NMSSM. If this particle is highly singlet, it will easily reach Dark Matter (DM) relic density and become an ideal particle for cold dark matter. So, the generic signatures of supersymmetric particles will involve missing energy due to the two neutral stable χ_1^0 s which escape the detector making the discovery of the a_1 at the LHC is challenging.

4 Conclusions

The SM-like Higgs boson mass of the range ~ 125 GeV can be accommodated in the framework of the NMSSM without much fine-tuning. In this model, by assuming CP-conservation, there are seven Higgs bosons: three CP-even, two CP-odd and a pair of charged Higgses. We have investigated the discovery potential of the lightest CP-odd Higgs boson a_1 produced through the gluon fusion production channel $gg \rightarrow a_1$ at the LHC with high center of mass energy, $\sqrt{s} = 14$ TeV in the context of the NMSSM. After computing the inclusive signal rates for $\tau^+\tau^-$, $\mu^+\mu^-$, $b\bar{b}$, $t\bar{t}$, $\gamma\gamma$, $Z\gamma$, $\chi_1^0\chi_1^0$ and $\chi_1^+\chi_1^-$ decay channels, we have found that the a_1 can have sizable signal rates in some regions of the NMSSM parameter space. While further studies about signal-to-background analysis are needed to make a final decision, we believe that the promising decay channels for the a_1 discovery at the LHC in the gluon fusion channel are $\tau^+\tau^-$, $\mu^+\mu^-$, $b\bar{b}$, $\gamma\gamma$, $Z\gamma$ channels.

Furthermore, we have noticed that the $\text{Br}(a_1 \rightarrow \gamma\gamma)$, $\text{Br}(a_1 \rightarrow Z\gamma)$, $\text{Br}(a_1 \rightarrow \chi_1^0\chi_1^0)$ and $\text{Br}(a_1 \rightarrow \chi_1^+\chi_1^-)$ can be dominant in some regions of the NMSSM parameter space. However, the $\text{Br}(a_1 \rightarrow \gamma\gamma)$ and $\text{Br}(a_1 \rightarrow Z\gamma)$ can only be dominant if the a_1 is highly singlet with a very small doublet component and both the channels $a_1 \rightarrow \chi_1^0\chi_1^0$ and $a_1 \rightarrow \chi_1^+\chi_1^-$ are kinematically closed. If the a_1 is a singlet-like and the channel $a_1 \rightarrow \chi_1^0\chi_1^0$ or $a_1 \rightarrow \chi_1^+\chi_1^-$ is kinematically open, the a_1 decays into $\gamma\gamma$ and into $Z\gamma$ are no longer dominant, in which case the a_1 decay into $\chi_1^0\chi_1^0$ or into $a_1 \rightarrow \chi_1^+\chi_1^-$ becomes substantial and dominant.

⁵The a_1 decay into lightest neutralino contributes to its invisible decay width.

Acknowledgments

This work is funded by Taibah University, KSA.

References

- [1] S. Chatrchyan *et al.* [CMS Collaboration], Phys. Lett. B **716**, 30 (2012).
- [2] G. Aad *et al.* [ATLAS Collaboration], Phys. Lett. B **716**, 1 (2012).
- [3] S. Chatrchyan *et al.* [CMS Collaboration], JHEP **1306**, 081 (2013).
- [4] G. Aad *et al.* [ATLAS Collaboration], Phys. Lett. B **726**, 88 (2013).
- [5] J. E. Kim and H. P. Nilles, Phys. Lett. B **138**, 150 (1984).
- [6] S. Weinberg, Phys. Lett. B **82**, 387 (1979).
- [7] C. H. Llewellyn Smith and G. G. Ross, Phys. Lett. B **105**, 38 (1981).
- [8] For reviews, see: e.g., U. Ellwanger, C. Hugonie and A. M. Teixeira, Phys. Rept. **496**, 1 (2010) (and references therein).
- [9] U. Ellwanger, JHEP **1203**, 044 (2012).
- [10] J. F. Gunion, Y. Jiang and S. Kraml, Phys. Lett. B **710**, 454 (2012).
- [11] S. F. King, M. Muhlleitner and R. Nevzorov, Nucl. Phys. B **860**, 207 (2012).
- [12] J. J. Cao, Z. X. Heng, J. M. Yang, Y. M. Zhang and J. Y. Zhu, JHEP **1203**, 086 (2012).
- [13] D. A. Vasquez, G. Belanger, C. Boehm, J. Da Silva, P. Richardson and C. Wymant, Phys. Rev. D **86**, 035023 (2012).
- [14] U. Ellwanger and C. Hugonie, Adv. High Energy Phys. **2012**, 625389 (2012).
- [15] R. Benbrik, M. Gomez Bock, S. Heinemeyer, O. Stal, G. Weiglein and L. Zeune, Eur. Phys. J. C **72**, 2171 (2012).
- [16] J. F. Gunion, Y. Jiang and S. Kraml, Phys. Rev. D **86**, 071702 (2012).
- [17] K. J. Bae, K. Choi, E. J. Chun, S. H. Im, C. B. Park and C. S. Shin, JHEP **1211**, 118 (2012).
- [18] K. Agashe, Y. Cui and R. Franceschini, JHEP **1302**, 031 (2013).
- [19] K. Choi, S. H. Im, K. S. Jeong and M. Yamaguchi, JHEP **1302**, 090 (2013).
- [20] K. Kowalska, S. Munir, L. Roszkowski, E. M. Sessolo, S. Trojanowski and Y. -L. S. Tsai, Phys. Rev. D **87**, 115010 (2013).

- [21] S. F. King, M. Muhlleitner, R. Nevzorov and K. Walz, Nucl. Phys. B **870**, 323 (2013).
- [22] T. Gherghetta, B. von Harling, A. D. Medina and M. A. Schmidt, JHEP **1302**, 032 (2013).
- [23] J. R. Ellis, J. F. Gunion, H. E. Haber, L. Roszkowski and F. Zwirner, Phys. Rev. D **39**, 844 (1989).
- [24] R. Dermisek and J. F. Gunion, Phys. Rev. D **76**, 095006 (2007).
- [25] G. Hiller, Phys. Rev. D **70**, 034018 (2004).
- [26] A. Arhrib, K. Cheung, T. J. Hou and K. W. Song, JHEP **0703**, 073 (2007).
- [27] F. Domingo, U. Ellwanger, E. Fullana, C. Hugonie and M. A. Sanchis-Lozano, JHEP **0901**, 061 (2009).
- [28] M. M. Almarashi and S. Moretti, Eur. Phys. J. C **71**, 1618 (2011).
- [29] M. M. Almarashi and S. Moretti, Phys. Rev. D **84**, 015014 (2011).
- [30] M. M. Almarashi and S. Moretti, Phys. Rev. D **83**, 035023 (2011).
- [31] M. M. Almarashi and S. Moretti, Phys. Rev. D **84**, 035009 (2011).
- [32] M. M. Almarashi and S. Moretti, Phys. Rev. D **85**, 017701 (2012).
- [33] M. M. Almarashi and S. Moretti, arXiv:1205.1683 [hep-ph].
- [34] D. G. Cerdeo, P. Ghosh, C. B. Park and M. Peir, JHEP **1402**, 048 (2014).
- [35] S. F. King, M. Muhlleitner, R. Nevzorov and K. Walz, Phys. Rev. D **90**, no. 9, 095014 (2014).
- [36] N. E. Bomark, S. Moretti, S. Munir and L. Roszkowski, JHEP **1502**, 044 (2015).
- [37] U. Ellwanger and C. Hugonie, JHEP **1605**, 114 (2016).
- [38] E. Conte, B. Fuks, J. Guo, J. Li and A. G. Williams, JHEP **1605**, 100 (2016).
- [39] M. Guchait and J. Kumar, Phys. Rev. D **95**, no. 3, 035036 (2017).
- [40] U. Ellwanger, J.F. Gunion and C. Hugonie, JHEP **0502**, 066 (2005).
- [41] U. Ellwanger and C. Hugonie, Comput. Phys. Commun. **175**, 290 (2006).
- [42] See <http://www.th.u-psud.fr/NMHDECAY/nmssmtools.html>.
- [43] A. Pukhov, arXiv:hep-ph/0412191.
- [44] S. Andreas, O. Lebedev, S. R. Sanchez and A. Ringwald, JHEP **1008**, 003 (2010).

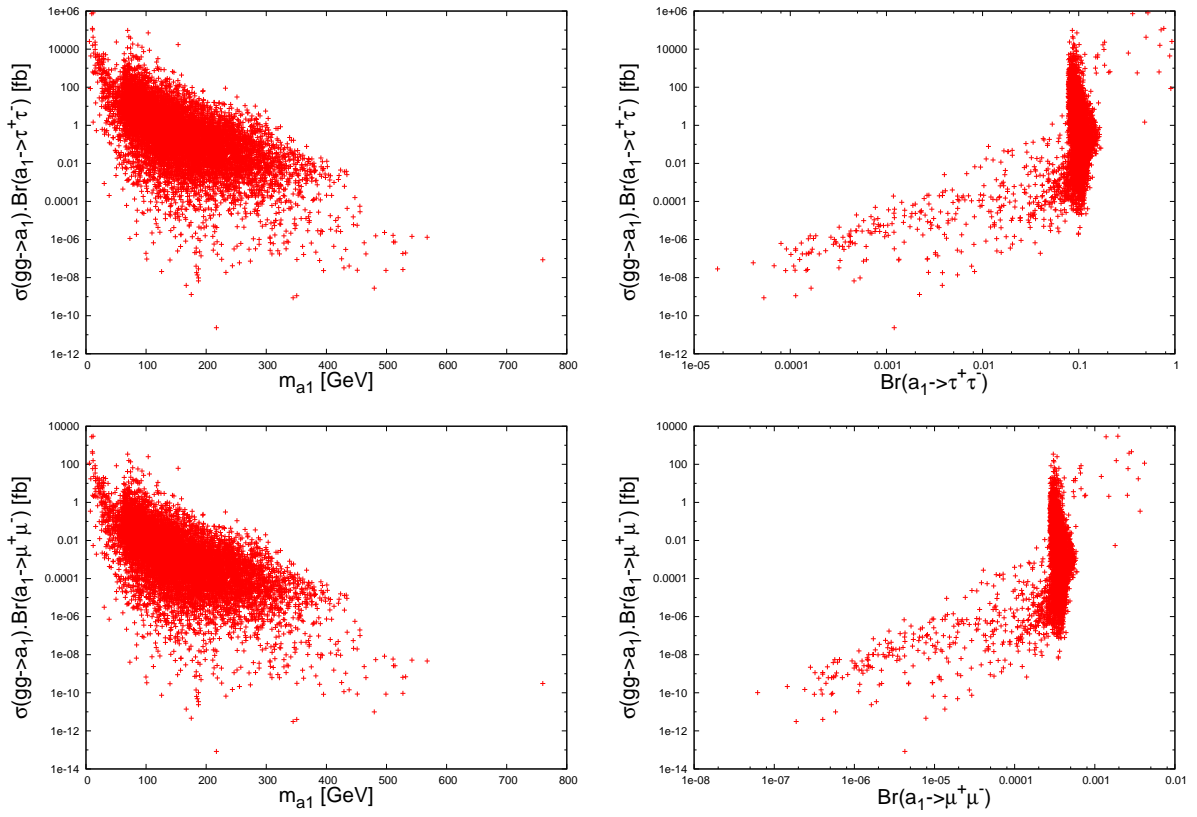


Figure 1: The production rates for $\sigma(gg \rightarrow a_1) \text{Br}(a_1 \rightarrow \tau^+ \tau^-)$ (top) and $\sigma(gg \rightarrow a_1) \text{Br}(a_1 \rightarrow \mu^+ \mu^-)$ (bottom) as functions of m_{a_1} (left) and of corresponding branching fractions (right).

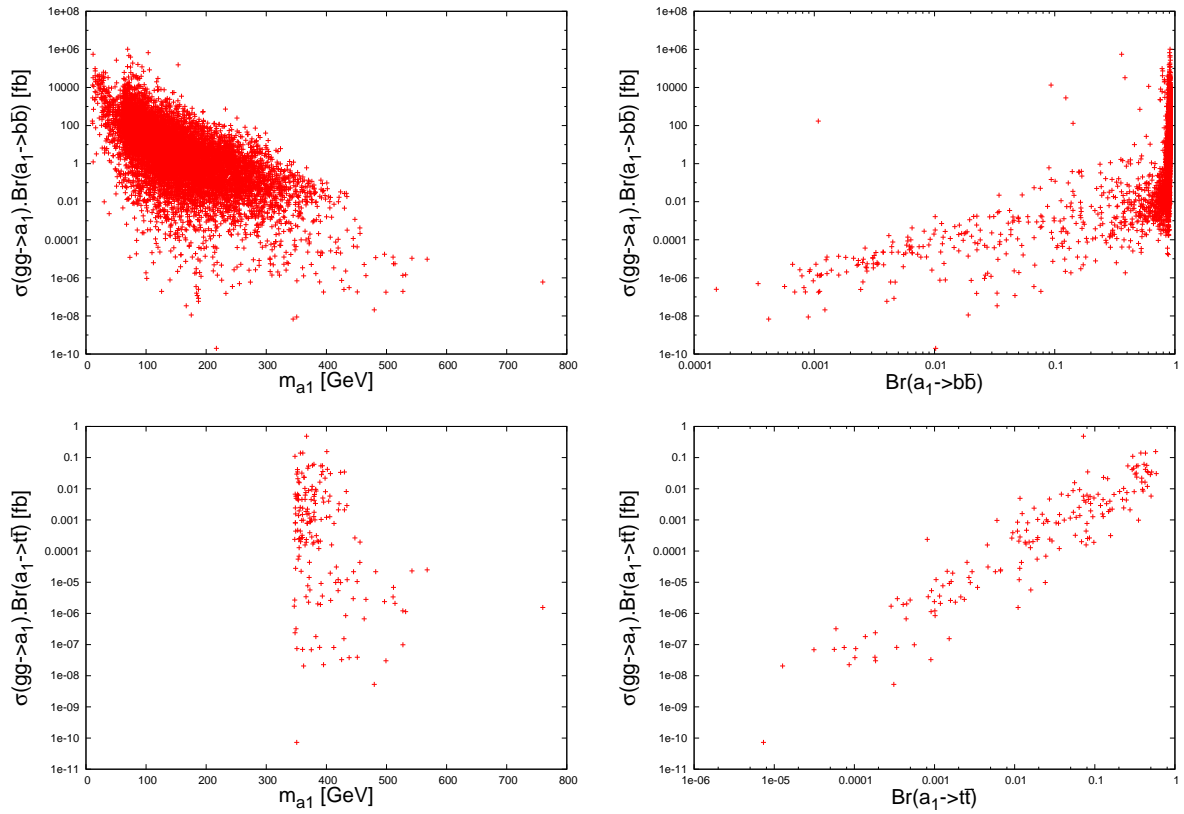


Figure 2: The production rates for $\sigma(gg \rightarrow a_1) \text{Br}(a_1 \rightarrow b\bar{b})$ (top) and $\sigma(gg \rightarrow a_1) \text{Br}(a_1 \rightarrow t\bar{t})$ (bottom) as functions of m_{a_1} (left) and of corresponding branching fractions (right).

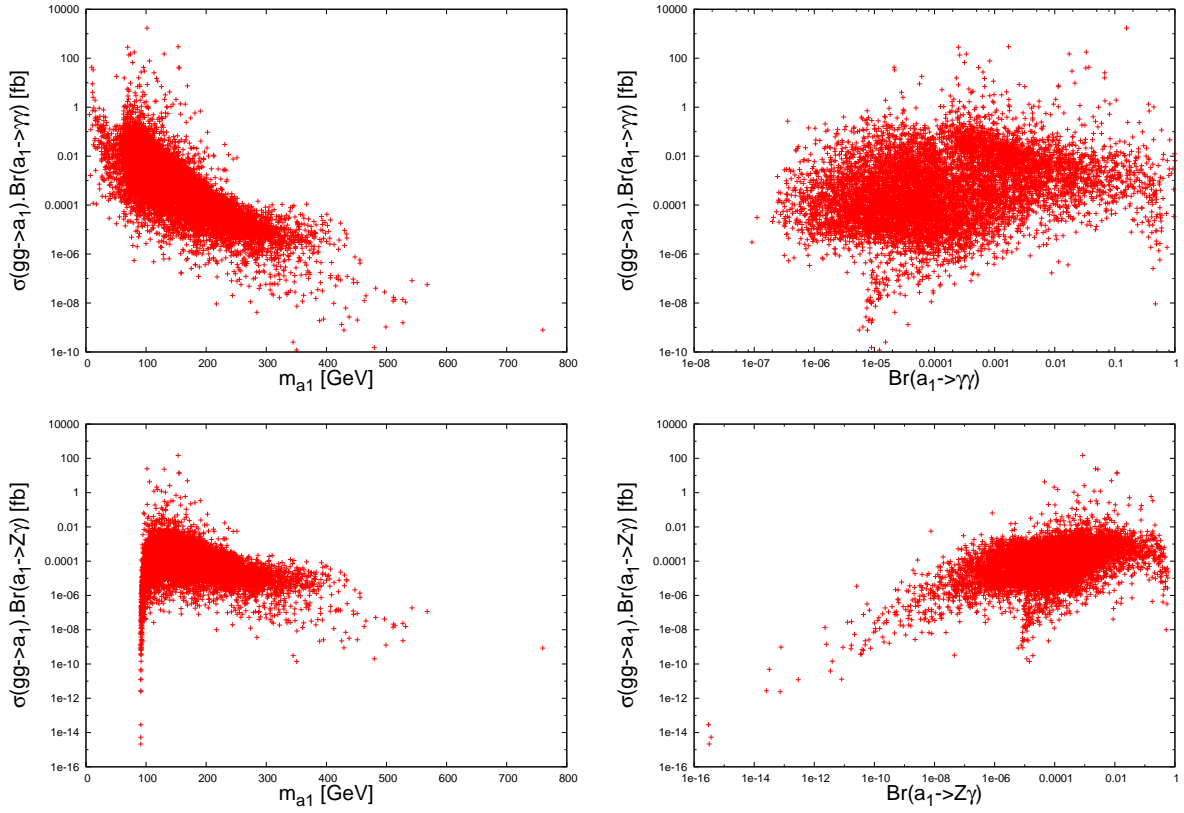


Figure 3: The production rates for $\sigma(gg \rightarrow a_1) \text{Br}(a_1 \rightarrow \gamma\gamma)$ (top) and $\sigma(gg \rightarrow a_1) \text{Br}(a_1 \rightarrow Z\gamma)$ (bottom) as functions of m_{a_1} (left) and of corresponding branching fractions (right).

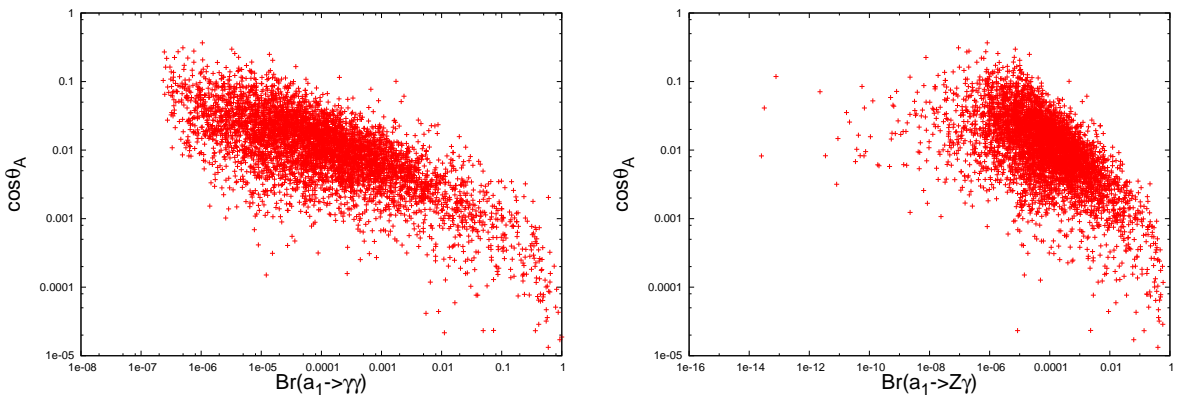


Figure 4: The correlations between the mixing angle $\cos\theta_A$ and the branching fractions $\text{Br}(a_1 \rightarrow \gamma\gamma)$ (left) and $\text{Br}(a_1 \rightarrow Z\gamma)$ (right).

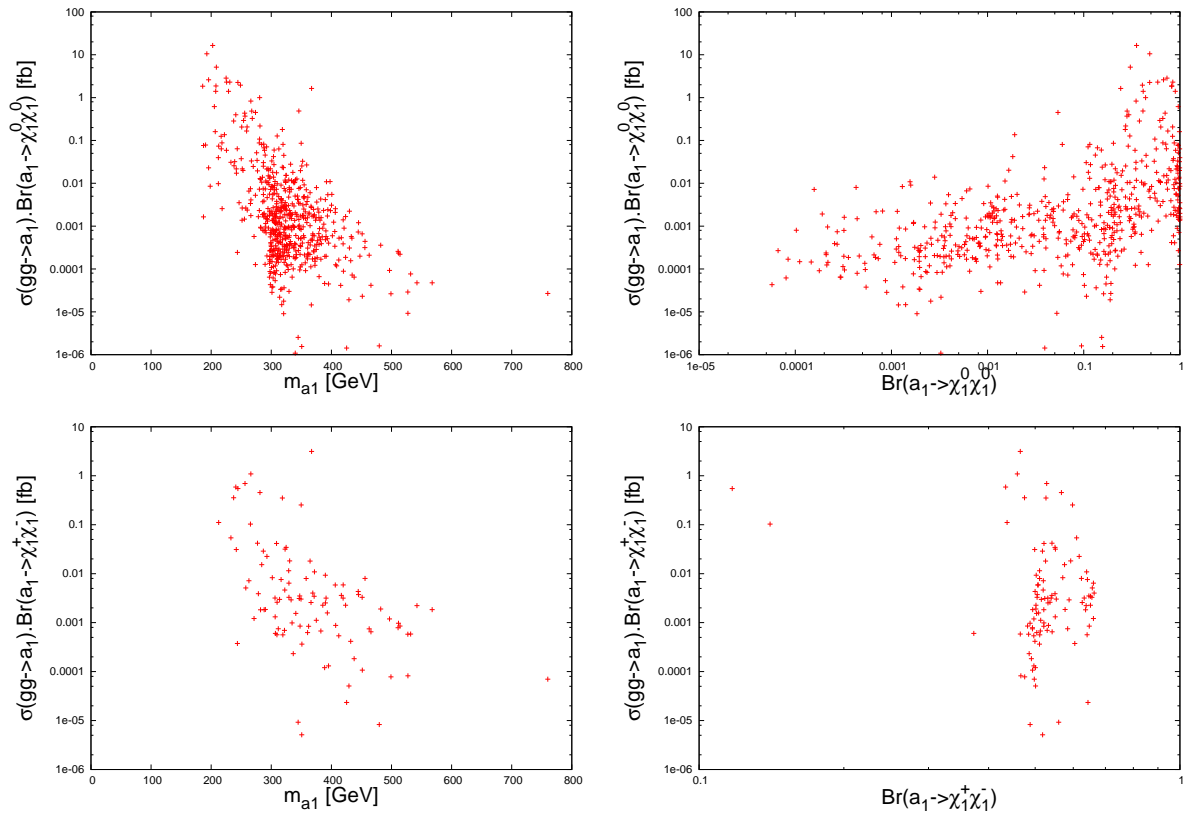


Figure 5: The production rates for $\sigma(gg \rightarrow a_1) \text{Br}(a_1 \rightarrow \chi_1^0 \chi_1^0)$ (top) and $\sigma(gg \rightarrow a_1) \text{Br}(a_1 \rightarrow \chi_1^+ \chi_1^-)$ (bottom) as functions of m_{a_1} (left) and of corresponding branching fractions (right).

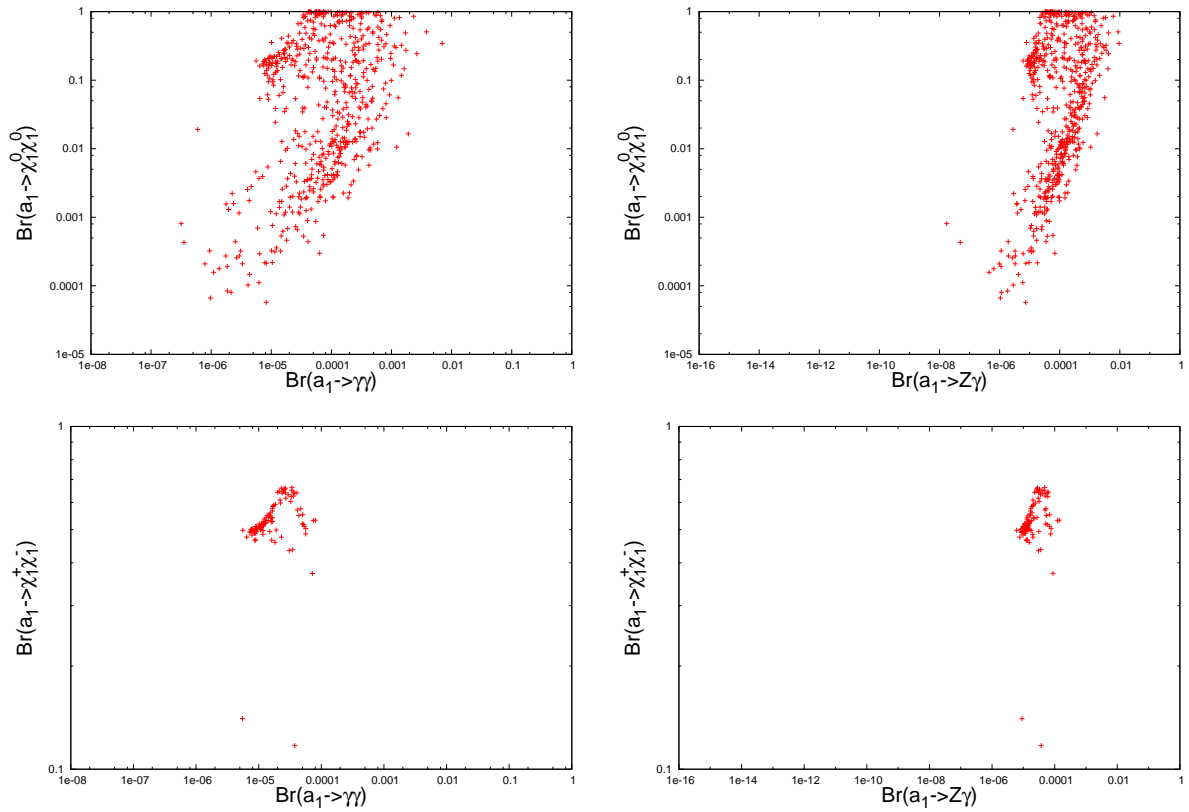


Figure 6: The branching fractions $\text{Br}(a_1 \rightarrow \chi_1^0 \chi_1^0)$ (top) and $\text{Br}(a_1 \rightarrow \chi_1^+ \chi_1^-)$ (bottom) plotted against the branching fractions $\text{Br}(a_1 \rightarrow \gamma\gamma)$ (left) and $\text{Br}(a_1 \rightarrow Z\gamma)$ (right).